Discovery of [18F]*N*-(2-(Diethylamino)ethyl)-6-fluoronicotinamide: A Melanoma Positron Emission Tomography Imaging Radiotracer with High Tumor to Body Contrast Ratio and Rapid Renal Clearance

Ivan Greguric,*,[†] Stephen R. Taylor,[†] Delphine Denoyer,[‡]
Patrice Ballantyne,[†] Paula Berghofer,[†] Peter Roselt,[‡]
Tien Q. Pham,[†] Filomena Mattner,[†] Thomas Bourdier,[†]
Oliver C. Neels,[‡] Donna S. Dorow,[‡] Christian Loc'h,[†]
Rodney J. Hicks,[‡] and Andrew Katsifis[†]

[†]*Radiopharmaceuticals Research Institute, Australian Nuclear Science and Technology Organisation, PMB 1, Menai NSW 2234, Sydney, Australia, and* [‡]*Centre for Molecular Imaging, The Peter MacCallum Cancer Centre, 12 St. Andrew's Place, East Melbourne, VIC 3002, Australia*

Abstract: The high melanoma uptake and rapid body clearance displayed by our series of [123I]iodonicotinamides prompted the development of [18F]*N*-(2-(diethylamino)ethyl)-6-fluoronicotinamide ([18F]**2**), a novel radiotracer for PET melanoma imaging. Significantly, unlike fluorobenzoates, [18F]fluorine incorporation on the nicotinamide ring is one step, facile, and high yielding. [18F]**2** displayed high tumor uptake, rapid body clearance via predominantly renal excretion, and is currently being evaluated in preclinical studies for progression into clinical trials to assess the responsiveness of therapeutic agents.

Skin cancer is the third most common human malignancy with 2−3 million new cases estimated across the world each year. Although melanoma accounts for only about 130000 of these, it is the most dangerous form and results in most of the deaths related to skin cancer. Survival largely depends on early detection and cure by surgical resection, as metastatic malignant melanoma is refractory to most therapies with a median survival of 6 months and a 5 year survival rate of less than 5%.[1] Despite a paucity of effective treatments currently, improved diagnostic methods have considerably decreased mortality rates.

A key feature of melanoma is the extensive pigmentation present in most tumor cells. Accordingly, this pigmentation is a very attractive target for both diagnosis and treatment. Radiopharmaceutical optimisation programs within our laboratory and other research groups have resulted in the development of iodobenzamides to target melanin with high selectivity and affinity. Radioiodinated (diethylaminoethyl)-iodobenzamides [123I]BZA[2] and [123I]BZA2[3] (Figure 1) demonstrated both high tumor uptake and good clearance from the body, making them excellent candidates for clinical studies. Our attempts to improve the tumor to background ratios and body clearance of iodobenzamides and other iodinated melanin binding compounds led to the development of the corresponding iodonicotinamide analogues including [123I]*N*-(2-(diethylamino)ethyl)-5-iodonicotinamide ([123I]MEL008).[4] Biological

studies have shown that the iodonicotinamide is readily taken up in melanoma tumors with subsequent melanin binding. The enhanced hydrophilicity of the pyridine nitrogen may also allow for a more rapid clearance from the remainder of the body via renal excretion. Furthermore, the nicotinamide structure is also amenable to direct nucleophilic substitution via a rapid, one-step synthesis, providing a high yielding method for the incorporation of the PET isotope [18F]fluorine onto these molecules.

Positron emission tomography (PET) has emerged as a valuable imaging tool due to its ability to provide high resolution and absolute quantitative uptake in tissue, with ease in background subtraction versus single photon emission computed tomography (SPECT) imaging. At present, 2-[18F]fluoro-2-deoxy-D-glucose [18F]FDG PET imaging of melanoma is the only PET clinical radiotracer used routinely to localize in melanoma tumors.[5] Although [18F]FDG is an effective tool for melanoma tumor detection, inflammation and infection decrease its specificity[6] and partial volume effects limits its sensitivity for small volume disease.[7]

Our objective was to incorporate fluorine within the *N*-alkyl-nicotinamide structure while retaining high melanin binding affinity, rapid whole body clearance of unbound tracer, stability, and ease of radiolabeling. As the nicotinamide structure is amenable to direct [18F]fluorination, we were able to construct a series of fluorine based nicotinamide compounds that retained the attractive biological properties displayed with our SPECT analogues.[4]

Here, we present the discovery of new PET [18F]fluoronicotinamide radiotracers prepared in one simple radiosynthetic step. One of them, [18F]*N*-(2-(diethylamino)-ethyl)-6-fluoronicotinamide ([18F]**2**), displayed rapid clearance, superior in vivo stability, and high target to nontarget ratio as demonstrated by animal PET imaging and biodistribution studies.

The authentic fluorine compounds **2**, **4**, **6**, and **8** and their precursors **1**, **3**, **5**, and **7** were readily prepared by condensation of a haloniconitic acid with the appropriate amine (Scheme 1). Hence, using the chloropyridine heterocycle, it was possible to introduce the [18F]fluorine atom directly onto the nicotinic ring by direct [18F]fluorination of the chloronicotinamide precursor and thus avoid a multistep radiosynthesis such as that reported for the preparation of *N*-(2-diethylaminoethyl)-4-[18F]fluorobenzamide ([18F]DAFBA).[8] [18F]Fluoronicotinamides [18F]**2**, [18F]**4**, [18F]**6**, and [18F]**8** were prepared within 40 min, including HPLC purification and formulation from their chloronicotinamide precursors. The resultant [18F]fluoronicotinamides were prepared in radiochemical yields of 35−55% (nondecay corrected). The radiotracers were produced in greater than 99% radiochemical purity and free of UV associated from the chloro-precursor, as demonstrated by QC analysis. The specific activity was in the range of 150−220 GBq/μmol and the radiochemical stability was maintained at >98% over 3−4 h in saline.

The biodistribution of the [18F]fluoronicotinamides was studied in two mice strains: C57BL/6J black mice bearing the B16F0 murine melanotic melanoma and BALB/c nude mice bearing the A375 human amelanotic tumor. In the B16F0 tumor, at 1 h, the uptake of the *N*-2-diethylaminoethyl

*To whom correspondence should be addressed. Phone: +61 2 9717 3759. Fax: +61 2 9717 9262. E-mail: ivg@ansto.gov.au.
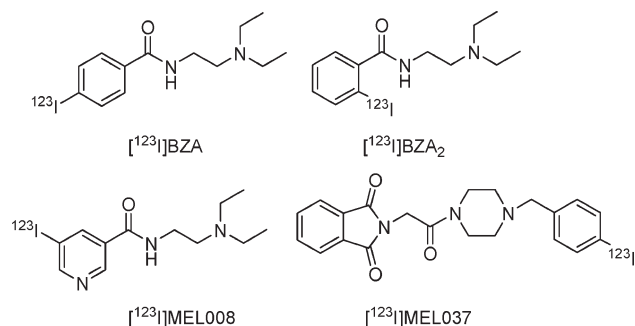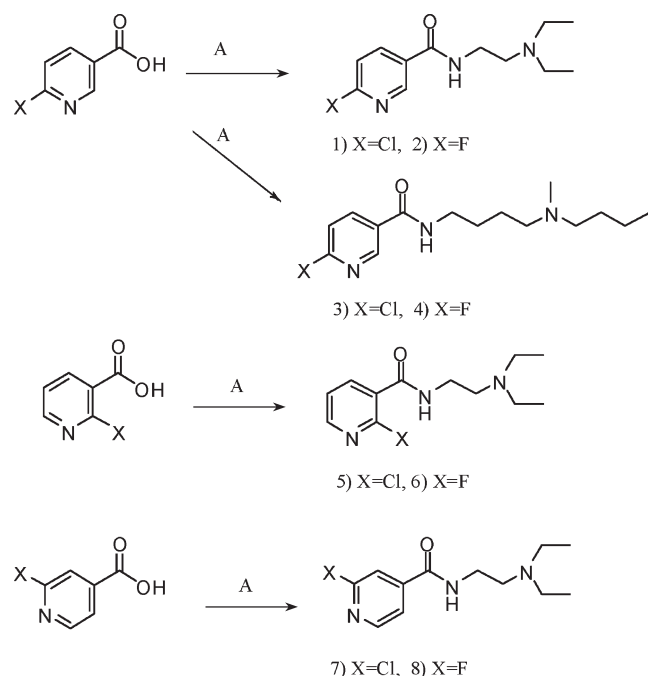
Figure 1. Benzamide and nicotinamide chemical structures.

Scheme 1. Synthesis of Nicotinamides (1−8)

^{a}(A) *N,N*-diethylethylenediamine or *N*-butyl-*N*-methylbutane-1,4-diamine, *N*-(3-dimethylaminopropyl)-*N'*-ethylcarbodiimide hydrochloride (EDCI), 1-hydroxybenzotriazole (HOBT), diisopropylethyl amine (DIPEA), DMF at RT for 20 h.

derivatives [^{18}F]**2**, [^{18}F]**6**, and [^{18}F]**8** were 2−3 times higher than the *N*-4-butyl(methyl)aminobutyl derivative [^{18}F]**4** (Table 1). Among them, the uptake of [^{18}F]**6** was the highest and displayed a maximum uptake at 3 h (17%ID/g), which decreased slowly over time. At 3 h, the uptake value for [^{18}F]**6** was at least 3-fold higher when compared to [^{18}F]DAFBA.[8]

Uptake of [^{18}F]fluoronicotinamides in the eyes of C57BL/6J black mice was significant (Figure 2) but similar to that of the analogous [^{123}I]iodoniconitamides[5] and other melanin binding compounds such as [^{123}I]2-(2-(4-(4-iodobenzyl)piperazin-1-yl)-2-oxoethyl) isoindoline-1,3-dione ([^{123}I]MEL037).[9] Uptake values in the B16F0 tumor and in the eyes of black mice at 3 h was more than 2 orders of magnitude greater than that observed in the BALB/c nude mice (which lack cutaneous and retinal pigmentation) bearing the A375 amelanotic tumor. The large uptake differences support the hypothesis that [^{18}F]fluoronicotinamides are involved in a specific interaction with melanin, which is inherent in the B16F0 tumor and the pigmented eye structure of C57BL/6J black mice.[4]

Bone uptake of [^{18}F]**2**, [^{18}F]**4**, and [^{18}F]**8** were low and the decrease paralleled those of peripheral organs and blood over time to reach values ranging between 0.5 and 1%ID/g at 6 h. Conversely for [^{18}F]**6**, uptake of radioactivity in the bone was
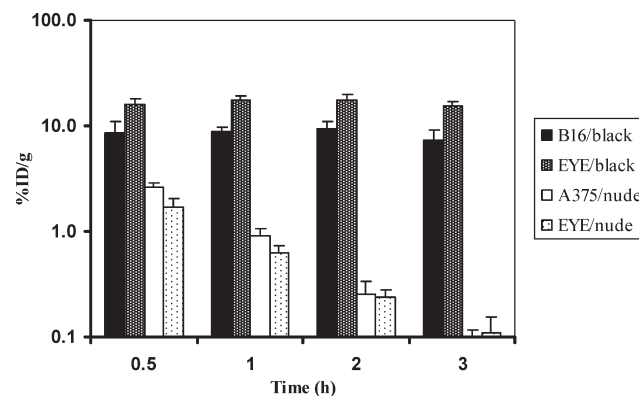

Figure 2. Radioactivity concentration in the tumor and eye of C57BL/6J black mice and BALB/c nude mice bearing the B16F0 melanotic and the A375 human amelanotic tumor, respectively, after the injection of [^{18}F]**2**. Results are expressed in percent of injected dose per gram (%ID/g ± SD; $n = 5$) in a logarithmic scale.

Table 1. Biodistribution of [^{18}F]Fluoronicotinamides^a

compound	time (h)	tumor	eye	lung	spleen	thyroid	stomach	intestine	bone
[^{18}F]**2**	0.25	7.0 ± 0.9	14.7 ± 0.5	5.6 ± 0.3	8.6 ± 2.0	5.5 ± 0.8	9.4 ± 1.1	5.4 ± 0.3	3.5 ± 0.2
	0.5	8.6 ± 2.4	16.0 ± 2.0	2.9 ± 0.4	7.2 ± 3.1	2.5 ± 0.3	6.6 ± 2.6	3.9 ± 0.5	2.1 ± 0.3
	1	8.4 ± 1.5	18.8 ± 2.4	1.6 ± 0.2	2.4 ± 1.4	3.3 ± 3.7	3.4 ± 0.9	2.1 ± 0.3	1.4 ± 0.3
	2	9.4 ± 1.6	17.3 ± 2.7	0.38 ± 0.04	1.8 ± 2.1	0.61 ± 0.33	1.5 ± 1.1	0.71 ± 0.11	0.58 ± 0.05
	3	7.8 ± 1.4	17.3 ± 3.1	0.25 ± 0.1	0.89 ± 1.6	0.49 ± 0.33	0.83 ± 0.55	0.54 ± 0.20	0.62 ± 0.19
	6	7.7 ± 2.3	15.6 ± 2.0	0.07 ± 0.03	0.47 ± 1.0	0.17 ± 0.07	0.19 ± 0.12	0.13 ± 0.06	0.52 ± 0.07
[^{18}F]**4**	0.25	4.0 ± 1.4	11.3 ± 2.6	12.1 ± 1.2	11.2 ± 1.1	10.2 ± 6.7	8.5 ± 3.1	8.2 ± 1.5	3.89 ± 0.5
	1	4.8 ± 1.1	12.7 ± 1.2	4.5 ± 0.5	7.4 ± 0.5	5.4 ± 2.9	3.3 ± 0.9	5.8 ± 0.7	2.0 ± 0.1
	3	5.3 ± 1.3	14.3 ± 2.1	3.1 ± 0.4	5.3 ± 1.2	2.9 ± 1.3	2.4 ± 0.9	4.2 ± 0.8	1.4 ± 0.3
	6	5.3 ± 1.5	15.8 ± 0.9	2.2 ± 0.1	4.1 ± 1.3	2.0 ± 0.4	1.8 ± 0.4	3.1 ± 0.5	1.0 ± 0.1
[^{18}F]**6**	0.25	10.6 ± 2.9	36.7 ± 7.1	5.0 ± 0.4	11.8 ± 3.2	4.5 ± 1.0	14.7 ± 1.6	7.8 ± 1.0	4.8 ± 0.3
	1	14.6 ± 5.1	38.0 ± 4.3	1.5 ± 0.3	9.2 ± 6.4	2.2 ± 0.4	6.8 ± 1.8	7.1 ± 0.3	3.4 ± 0.2
	3	17.3 ± 1.7	36.3 ± 2.8	0.35 ± 0.08	2.5 ± 3.5	2.1 ± 0.4	1.9 ± 1.4	7.1 ± 1.0	4.6 ± 0.2
	6	4.8 ± 0.7	27.4 ± 5.8	0.20 ± 0.03	0.5 ± 0.7	3.2 ± 2.9	0.7 ± 0.9	3.6 ± 0.5	5.6 ± 0.2
[^{123}I]**8**	0.25	7.0 ± 0.9	17.3 ± 2.1	5.7 ± 0.4	10.3 ± 2.6	4.8 ± 0.4	13.2 ± 1.6	7.0 ± 0.3	4.0 ± 0.3
	1	12.2 ± 3.3	23.7 ± 1.2	1.8 ± 0.3	3.2 ± 1.0	2.2 ± 0.4	5.3 ± 1.5	2.9 ± 0.2	1.5 ± 0.1
	3	8.8 ± 3.0	18.8 ± 1.2	0.37 ± 0.06	2.3 ± 2.7	1.5 ± 0.5	0.82 ± 0.36	0.72 ± 0.18	0.77 ± 0.13
	6	7.2 ± 2.5	16.5 ± 1.8	0.14 ± 0.03	1.3 ± 2.6	1.0 ± 0.4	0.30 ± 0.15	0.23 ± 0.05	0.43 ± 0.07

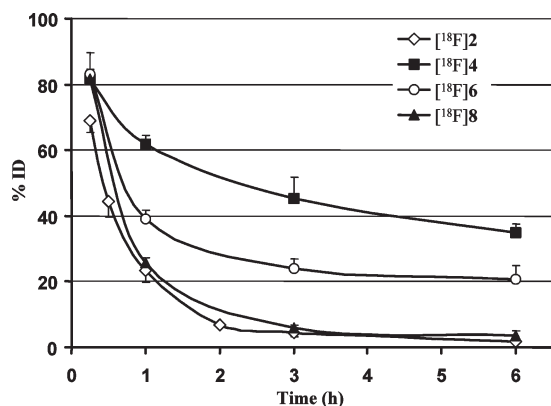^{a} Data are the means of %ID/g of tissue ± SD; $n = 5$. B16F0 melanoma tumor in C57BL/6J mice.

Figure 3. Activity remaining in the body after the injection of [^{18}F]fluoronicotinamide series in C57BL/6J black mice with B16F0 tumor. Results are expressed in percent of injected dose (%ID ± SD; $n = 5$).

increasing over time to reach 6%ID/g at 6 h. A comparison of bone uptake with the heterocyclic structure suggests that the 2-fluoroisonicotinamide [^{18}F]**8** and 6-fluoronicotinamide [^{18}F]**2** compounds are very stable with respect to in vivo defluorination. However, uptake of activity in the bone for [^{18}F]**6** suggests a greater propensity for the 2-fluoronicotin-amide structure to defluorinate in vivo. Our lead, [^{18}F]**2**, displayed the least bone uptake (0.5%ID/g) at 6 h and is comparable to that reported for [^{18}F]DAFBA.[8] Further examination of the in vivo stability of [^{18}F]**2** indicated that more than 90% of activity in tumor, eyes, and urine and 70% in plasma was unchanged [^{18}F]**2** at 2 h. These observations and the low bone uptake suggest that [^{18}F]**2** is stable in rodents in vivo for at least 2 h.

The activity versus time in C57BL/6J black mice after [^{18}F]fluoronicotinamide injection is shown in Figure 3. As with the iodonicotinamides,[4] the main excretion route of fluoronicotinamides from the animals was found to be renal. The clearance from the body was more rapid for the *N*-2-diethylaminoethyl derivatives [^{18}F]**2**, [^{18}F]**6**, and [^{18}F]**8** than the *N*-4-butyl(methyl)aminobutyl analogue [^{18}F]**4**. Additionally, 95% of the 6-fluoronicotinamide [^{18}F]**2** had cleared from the body over 3 h, a clearance rate 5 times faster than that of the 2-fluoronicotinamide [^{18}F]**6**.

Previous studies have indicated that the excretion rate and routes of iodobenzamides[3] and iodonicotinamides[4] are influenced by the substitution groups on the nitrogen amide, length, and substitution of alkyl chains and the type and substitution pattern on the aromatic group. Using the less lipophilic *N*-2-diethylaminoethyl alkyl chain and incorporating the halo-pyridine ring system, we were able to increase the overall hydrophilic character of the alkyl-fluoroniconitamides. This was confirmed with [^{18}F]**2**, [^{18}F]**6**, and [^{18}F]**8** displaying the lowest lipophilicity value (log$P_{7.5}$: 0.94−1.2) compared to [^{18}F]**4** (log$P_{7.5}$: 1.5). With these considerations, it appears that [^{18}F]**2** with high tumor uptake and rapid clearance displayed the highest target to nontarget ratio of 40 at 3 h. This [^{18}F]**2** ratio suggests an enhanced opportunity for the visualization of melanoma tumors in clinical PET imaging.

The high sensitivity and specificity of [^{18}F]**2** for melanoma tumors is illustrated by PET imaging and ex vivo autoradiography. The whole body and transaxial section PET images display the clear visualization of a B16F0 tumor allograft at 1 h post tracer injection of [^{18}F]**2** in Figure 4 with a high tumor to background ratio. An [^{18}F]**2** signal was also visible in the

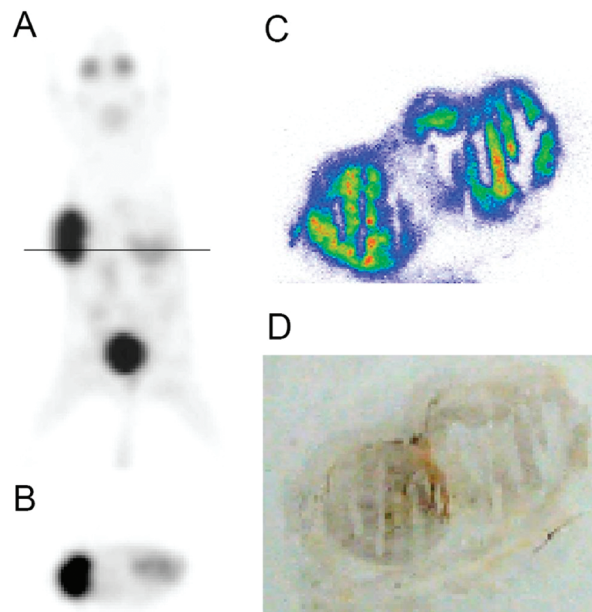**Figure 4.** [^{18}F]**2** PET image analysis of murine melanoma. (A) Whole body and (B) transaxial PET images of a C57BL/J6 black mouse bearing a B16F0 tumor allograft (right flank) at 1 h post-injection of [^{18}F]**2**. (C) Autoradiographic and (D) photographic images of [^{18}F]**2** uptake in melanotic areas of a B16F0 tumor frozen section from a 1 h autoradiographic acquisition of [^{18}F]fluorine disintegrations.

bladder at the 1 h time point, confirming the clearance of this tracer through the urinary system.

Immediately after PET imaging, frozen sections of tumor tissue were subjected to high resolution autoradiography and the resultant images are shown in Figure 4. Areas of melanin pigmented tissue visible in digital photographs of the tissue sections coincide with intense [^{18}F]**2** radiographic signal in the tumor section of the autoradiographic image.

In summary, we prepared a series of fluoronicotinamide analogues with enhanced melanin binding and uptake, rapid clearance, and high in vivo stability. It was found that the fluoronicotinamide structures are not only excellent bioisosteres of previously reported halogenated benzamides but the nicotinamides also possess superior radiolabeling properties. Among the series, nicotinamides bearing the lipophilic amine *N*-butyl-*N*-methylbutane-1,4-diamine [^{18}F]**4** and the 2-fluoronicotinamide heterocycle [^{18}F]**6** gave poor relative in vivo clearance, while evidence suggests that [^{18}F]**6** experiences significant in vivo defluorination. Coupling 6-fluoronicotinic acid to *N*,*N*-diethylethylenediamine led to the discovery of [^{18}F]**2**, which possessed the highest target to nontarget ratio, high in vivo stability, and rapid whole body clearance.

These studies indicate that [^{18}F]**2** will be a superior PET tracer for clinical staging due to higher lesion contrast that will allow more sensitive detection of small metastases and thereby enable more accurate selection and planning of treatment as well as better therapeutic monitoring in melanoma compared to existing standards including [^{18}F]FDG (manuscript in preparation).

Supporting Information Available: Details of synthesis, characterization, radiosynthesis, lipophilicity, biodistribution,

imaging, metabolite analysis, and audioradiography. This material is available free of charge via the Internet at http://pubs.acs.org.

References

(1) Cummins, D. L.; Cummins, J. M.; Pantle, H.; Silverman, M. A.; Leonard, A, L.; Chanmugam, A. Cutaneous malignant melanoma. *Mayo Clin. Proc.* **2006**, *81*, 500–507.

(2) Michelot, J. M.; Moreau, M. F.; Veyre, A. J.; Bonafous, J. F.; Bacin, F. J.; Madelmont, J. C.; Bussiere, F.; Souteyrand, P. A.; Mauclaire, L. P.; Chossat, F. M.; Papon, J. M.; Labarre, P. G.; Kauffmann, Ph.; Plagne, R. J. Phase II scintigraphy clinical trial of malignant melanoma and metastases with iodine-123-*N*-(2-diethylaminoethyl 4-iodobenzamide). *J. Nucl. Med.* **1993**, *34*, 1260–1266.

(3) Sillaire-Houtmann, I.; Bonafous, J.; Veyre, A.; Mestas, D.; D'Incan, M.; Moins, N.; Kemeny, J. L.; Chossat, F.; Bacin, F. Phase 2 clinical study of ^{123}I-*N*-(2-diethylaminoethyl)-2-iodobenzamide in the diagnostic of primary and metastatic ocular melanoma. *J. Fr. Ophthalmol.* **2004**, *27*, 34–39.

(4) Liu, X.; Pham, T. Q.; Berghofer, P.; Chapman, J.; Greguric, I.; Mitchell, P.; Mattner, F.; Loc'h, C.; Katsifis, A. Synthesis and evaluation of novel radioiodinated nicotinamides for malignant melanoma. *Nucl. Med. Biol.* **2008**, *35*, 769–781.

(5) Belhocine, T. Z.; Scott, A. M.; Even-Sapir, E.; Urbain, J. L.; Essner, R. Role of nuclear medicine in the management of cutaneous malignant melanoma. *J. Nucl. Med.* **2006**, *47*, 957–967.

(6) Hafner, J.; Schmid, M. H.; Kempf, W.; Burg, G.; Kunzi, E.; Meuli-Simmen, C.; Neff, P.; Meyer, V.; Mihic, D.; Garzoli, E.; Jungius, K. P.; Seifert, B.; Dummer, R.; Steinert, H. Baseline staging in cutaneous malignicant melanoma. *Br. J. Dermatol.* **2004**, *150*, 677–686.

(7) Dimitrakopoulou-Strauss, A.; Strauss, L. G.; Burger, C. Quantitative PET studies in pretreated melanoma patients: a comparison of 6-[^{18}F]fluoro-L-dopa with ^{18}F-FDG and ^{15}O-water using compartment and noncompartment analysis. *J. Nucl. Med.* **2001**, *42*, 248–256.

(8) Garg, S.; Kothari, K.; Thopate, S. R.; Doke, A. K.; Garg, P. K. Design, synthesis, and preliminary in vitro and in vivo evaluation of *N*-(2-diethylaminoethyl)-4-[^{18}F]fluorobenzamide ([^{18}F]-DAFBA): a novel potential PET probe to image melanoma tumors. *Bioconjugate Chem.* **2009**, *20*, 583–590.

(9) Pham, T. Q.; Berghofer, P.; Liu, X.; Greguric, I.; Dikic, B.; Ballantyne, P.; Mattner, F.; Nguyen, V.; Loc'h, C.; Katsifis, A. Preparation and biologic evaluation of a novel radioiodinated benzylpiperazine, ^{123}I-MEL037, for malignant melanoma. *J. Nucl. Med.* **2007**, *48*, 1348–1356.